





Article

Experimental Study for the Sorption and Diffusion of Supercritical Carbon Dioxide into Polyetherimide

Wei-Heng Huang ^{1,†}, Pei-Hua Chen ^{2,3,†}, Chin-Wen Chen ^{4,*} , Chie-Shaan Su ⁵ , Muoi Tang ¹, Jung-Chin Tsai ⁶, Yan-Ping Chen ⁷  and Feng-Huei Lin ² 

¹ Department of Chemical and Materials Engineering, Chinese Culture University, Taipei 111396, Taiwan; a6580800@ulive.pccu.edu.tw (W.-H.H.); muoitang@ulive.pccu.edu.tw (M.T.)

² Department of Biomedical Engineering, National Taiwan University, Taipei 106319, Taiwan; 16185@s.tmu.edu.tw (P.-H.C.); double@ntu.edu.tw (F.-H.L.)

³ Department of Orthopedics, Shuang Ho Hospital, Taipei Medical University, New Taipei City 235041, Taiwan

⁴ Department of Molecular Science and Engineering, National Taipei University of Technology, Taipei 106344, Taiwan

⁵ Department of Chemical Engineering and Biotechnology, National Taipei University of Technology, Taipei 106344, Taiwan; cssu@ntut.edu.tw

⁶ Department of Chemical Engineering, Ming Chi University of Technology, New Taipei City 243303, Taiwan; jctsai@mcut.edu.tw

⁷ Department of Chemical Engineering, National Taiwan University, Taipei 106319, Taiwan; ypchen@ntu.edu.tw

* Correspondence: cwchen@ntut.edu.tw

† These authors contributed equally to this work.

Abstract: Supercritical carbon dioxide (SCCO₂) is a non-toxic and environmentally friendly fluid and has been used in polymerization reactions, processing, foaming, and plasticizing of polymers. Exploring the behavior and data of SCCO₂ sorption and dissolution in polymers provides essential information for polymer applications. This study investigated the sorption and diffusion of SCCO₂ into polyetherimide (PEI). The sorption and desorption processes of SCCO₂ in PEI samples were measured in the temperature range from 40 to 60 °C, the pressure range from 20 to 40 MPa, and the sorption time from 0.25 to 52 h. This study used the ex situ gravimetric method under different operating conditions and applied the Fickian diffusion model to determine the mass diffusivity of SCCO₂ during sorption and desorption processes into and out of PEI. The equilibrium mass gain fraction of SCCO₂ into PEI was reported from 9.0 wt% (at 60 °C and 20 MPa) to 12.8 wt% (at 40 °C and 40 MPa). The sorption amount increased with the increasing SCCO₂ pressure and decreased with the increasing SCCO₂ temperature. This study showed the crossover phenomenon of equilibrium mass gain fraction isotherms with respect to SCCO₂ density. Changes in the sorption mechanism in PEI were observed when the SCCO₂ density was at approximately 840 kg/m³. This study qualitatively performed FTIR analysis during the SCCO₂ desorption process. A CO₂ antisymmetric stretching mode was observed near a wavenumber of 2340 cm⁻¹. A comparison of loss modulus measurements of pure and SCCO₂-treated PEI specimens showed the shifting of loss maxima. This result showed that the plasticization of PEI was achieved through the sorption process of SCCO₂.

Keywords: supercritical carbon dioxide; polyetherimide; sorption; Fickian diffusion model; diffusivity



Citation: Huang, W.-H.; Chen, P.-H.; Chen, C.-W.; Su, C.-S.; Tang, M.; Tsai, J.-C.; Chen, Y.-P.; Lin, F.-H.

Experimental Study for the Sorption and Diffusion of Supercritical Carbon Dioxide into Polyetherimide.

Molecules **2024**, *29*, 4233. <https://doi.org/10.3390/molecules29174233>

Academic Editor: Ivan Gitsov

Received: 30 July 2024

Revised: 22 August 2024

Accepted: 30 August 2024

Published: 6 September 2024



Copyright: © 2024 by the authors. Licensee MDPI, Basel, Switzerland. This article is an open access article distributed under the terms and conditions of the Creative Commons Attribution (CC BY) license (<https://creativecommons.org/licenses/by/4.0/>).

1. Introduction

Studying the sorption behavior of gas or penetrant in synthetic polymers is of great importance for fundamental research and technological applications and has been discussed in recent reviews [1–4]. Many important developments exist in applying polymer materials with low- or high-pressure carbon dioxide (CO₂), as described below. Polymer-containing materials have been used in zero-emission pathways for CO₂ capture or CO₂ transport chain, where gas sorption, selectivity, and polymer modification are interesting topics [5,6]. Regarding material processing, the sorption of supercritical CO₂ (SCCO₂) into polymers

is of great importance for the surface modification or foaming of substrates. SCCO₂ has widely been used in the above processing of polymer materials due to its good diffusion coefficient, low viscosity, and safety considerations [7,8]. Modifiers are injected into the polymer substrate through sorption of SCCO₂, which is the first step to be considered when controlling polymer properties such as surface grafting. Foaming and surface modification of polymers using SCCO₂ as the blowing agent or as a green solvent for reaction medium to produce medical or biocompatible value-added products have recently been reviewed [9,10], where SCCO₂ solubility data are essentially needed. Surface graft polymerization is an example of minimizing protein fouling in protein recovery application [11] or enhancing the hydrophilicity of versatile commodity polymers [12]. Processing polymeric materials requires information on the phase equilibrium and transport properties of SCCO₂ in the polymer matrix. The polymer modification strategy as an oxygenator in extracorporeal respiratory circulation or grafting hydrophilic 2-hydroxyethyl methacrylate (HEMA) monomer onto polyacrylonitrile (PAN) polymer substrate to obtain ultrafiltration biomedical materials requires information on the sorption and diffusion between SCCO₂ and polymers [10,13,14].

The sorption and transport of SCCO₂ in polymers was recently studied theoretically by Ricci et al. [15]. Experimental studies for the sorption amounts and diffusion coefficients of SCCO₂ in various polymer substrates have been reported in the literature [16–25]. The recent literature shows that the availability of thermodynamic and transport properties (e.g., solubility and diffusivity) of SCCO₂–polymer mixtures is limited [15], and more experimental data on various polymer systems are still needed. The gravimetric technique is the most common method used to measure the amount and rate of SCCO₂ sorption into polymers. The gravimetric method records the rate of weight change in a polymer sample after soaking in SCCO₂ at a given temperature, pressure, and sorption time. The Fickian mass transfer model then analyzes the recorded data to evaluate the diffusivity of SCCO₂ into or out from the polymer or copolymer membrane samples [24,25]. The results of these fundamental studies supply essential information for SCCO₂-assisted polymer processing, as shown in a previous review article [26]. Fundamental data on the sorption and desorption diffusivities of SCCO₂ in many unstudied polymers, copolymers, or polymer blend systems are still needed. These data can enable new applications of polymer modification to produce value-added products such as drug delivery foams and films, biomedical devices, and biodegradable materials in tissue engineering [4].

In this study, we report the experimental measurement results for the sorption and diffusion of SCCO₂ into polyetherimide (PEI). PEI is an amorphous thermoplastic polymer with chemical stability and ductile properties for various applications. It has been illustrated that PEI is a candidate for biomedical usage, such as intraocular lenses, biosensors, or neuroprostheses [27]. The PEI backbone can be modified through wet chemistry to prepare membranes for artificial organs. Feng et al. [28] have presented using SCCO₂/ethanol co-foaming technology to fabricate PEI bead foams with three-dimensional geometry for special engineering plastic materials in high-tech industries. The production of PEI nanofoams has been presented by Aher et al. [29] using SCCO₂ as the blowing agent. They studied the sorption of SCCO₂ at 20 MPa into the commercially available PEI sheets. The diffusion coefficients at 0 °C and room temperature (23 °C) were experimentally determined. The equilibrium concentration of SCCO₂ absorbed in PEI has also been studied by Zhou et al. [30] at pressures from 6 to 10 MPa. They conducted the SCCO₂ saturation study in PEI before fabricating the PEI nanofoams with high strength, toughness, and good thermal resistivity. A process map for the foaming temperature and absorbed SCCO₂ concentration was developed.

This study aimed to investigate the novel sorption and diffusion of SCCO₂ in PEI using the *ex situ* gravimetric method within a pressure and temperature range (pressure studied at 20, 30, and 40 MPa; temperature studied at 40, 50, and 60 °C). The mass diffusivities were evaluated based on the Fickian diffusion model using experimentally measured data under various experimental conditions. The effects of temperature and pressure on the

sorption mass gain fractions and sorption diffusivities are discussed. The equilibrium sorption mass gain fractions depended on the density of SCCO₂, where the crossover phenomenon of the absorption isotherms was determined and explained. The desorption behavior of SCCO₂ from PEI was analyzed through Fourier-transform infrared (FTIR) spectroscopy, demonstrating the antisymmetric stretching mode of CO₂ trapped in PEI at different desorption times. The plasticization effect of PEI by absorbed SCCO₂ was examined using loss modulus measurements, where the measured results of loss maxima were illustrated. These basic data provide helpful information for future applications of PEI, such as being a prime candidate for medical tools [27,31] with good biocompatibility and becoming an integral component of interior panels, electrical enclosures, and aerospace industry [9] due to its flame retardancy and weight reduction potential.

2. Results

2.1. Determination of the Sorption and Desorption Diffusivities of SCCO₂ in PEI

For the sorption experiments in this study, we used the ex situ gravimetric method, and the detailed description of the experimental apparatus and procedures is shown in Section 3.2. In the experiments, we measured the desorption mass gain fraction (M_d), determined the sorption mass gain fraction (M_s) and the equilibrium sorption mass gain fraction (M_∞) at specific operation conditions. Figure 1 presents the plot of the desorption mass gain fraction M_d against the square root of desorption time t_d , where the sorption experiments were performed at 60 °C, 30 MPa, and various sorption time parameters t_s . The different desorption lines shown in Figure 1 were obtained from different PEI sample sheets during the experiments. Detailed experimental procedures are described in Section 3.2, Apparatus and procedures. It is stated in Section 3.3, Data analysis method, that the linear relations between M_d with the square root of the desorption time (t_d)^{1/2}, as represented by Equation (5), demonstrated that the Fickian diffusion model [32] was suitable to fit the experimental data at a short desorption interval. The mass gain fraction of SCCO₂ (M_s) absorbed into the PEI sample at the specific sorption time t_s parameter was determined as the intercept by extrapolating each desorption line to zero desorption time. This extrapolation method is described in Section 3.2, Apparatus and procedures.

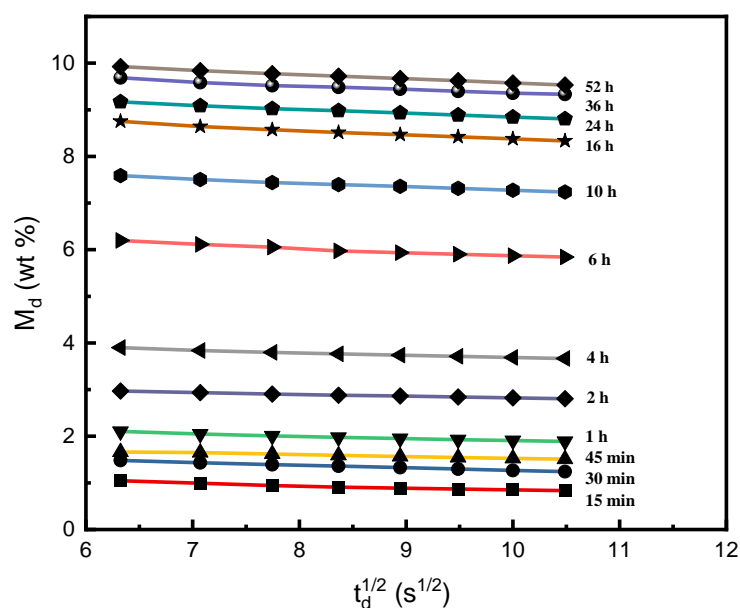


Figure 1. Plot of the desorption mass gain fraction (M_d) against the square root of the desorption time (t_d)^{1/2} for PEI, where the sorption experiments were performed at 60 °C, 30 MPa, and various sorption time parameters t_s from 15 min to 52 h.

By repeating the desorption experiments using the ex situ gravimetric method under different operating temperatures, pressures, and various sorption time parameters, the sorption mass gain fractions (M_s) under specific sorption conditions were obtained. Figure 2 shows the results at 60 °C and three sorption isobars at 20, 30, and 40 MPa, respectively. For PEI samples with a thickness of 0.6 mm, the SCCO₂ sorption amount leveled off after reaching equilibrium around 50 h under all experimental conditions. The leveled-off point yielded experimental data for the equilibrium mass gain fraction, M_∞ . The regression results of the sorption curves for each isobar were satisfactory and are displayed in Figure 2.

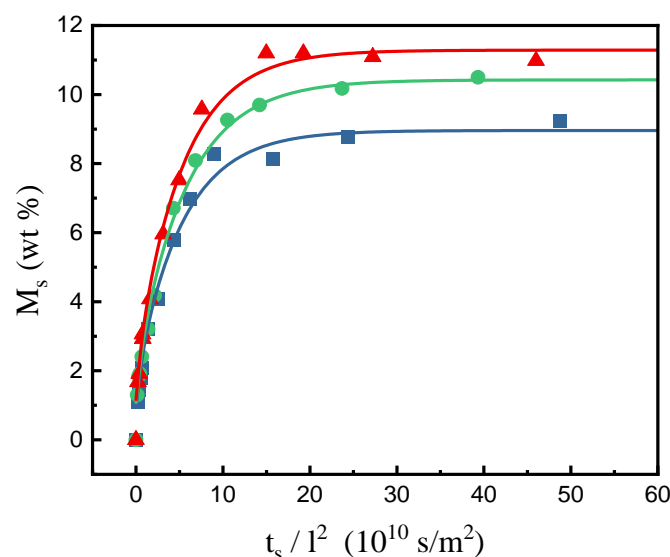


Figure 2. The mass gain fractions of PEI at 60 °C and various pressures: ■, 20 MPa; ●, 30 MPa; ▲, 40 MPa. The curves were obtained by regression on the experimental data.

The M_∞ values were determined by plateauing the isobaric M_s data, and these values support the necessary information for further polymer processing, such as foaming or grafting. This study also obtained similar experimental results for three isobars at 40 and 50 °C, respectively. All these experimental data were used to evaluate the sorption diffusivity D_s and desorption diffusivity D_d for long sorption time and short desorption time, respectively. A linear plot method was employed to determine the diffusivity data described in Equations (4) and (5) in Section 3.3. Table 1 lists the diffusivity results for SCCO₂ sorption and desorption in PEI for three isobars at 40, 50, and 60 °C, respectively. The density data listed in Table 1 for pure CO₂ were retrieved from the NIST database [33]. It can be observed from Table 1 that at the lowest temperature and highest pressure of 40 °C and 40 MPa, the highest sorption mass gain fraction of SCCO₂ in PEI is 12.8 wt%. The M_∞ values measured in this study are consistent with values reported in the literature [29], which reported that M_∞ for PEI was approximately 10 wt% at 20 MPa and 45 °C.

Figure 3 shows a graphical representation of the equilibrium sorption mass gain fraction (M_∞) for three isotherms at different pressures, including all experimental data in this study. The equilibrium sorption mass gain fraction at a constant temperature increased with the increasing pressure. Taking the 60 °C isotherm as an example, M_∞ of 7.9 wt% was obtained at a low pressure of 13.5 MPa, and M_∞ of 14.1 wt% was obtained at a high pressure of 58.3 MPa. Figure 3 also indicates that M_∞ decreased with increasing temperature at constant pressure. The literature mentions that the spectroscopic results showed that CO₂ has specific interactions with various polymers. This interaction has exothermic properties, resulting in reduced solubility of CO₂ in the polymer at higher temperatures under isobaric conditions [20,34–36]. The same trend was found in the literature on SCCO₂ sorption in polycarbonate (PC) and polysulfone (PSF) [24,25], as well as poly(vinyl chloride) (PVC) [37]. Compared with the experimental results in the literature, the M_∞ values of polycarbonate (PC) polymer were relatively higher than those of polysulfone (PSF) [24,25] and PEI. Under

the same temperature and pressure conditions, the M_{∞} values of PEI measured in this study are close to those of PSF. The interactions between CO_2 and functional groups in various polymer matrices may be responsible for these findings. The interaction between CO_2 and the carbonyl groups of PC increased the amount of CO_2 absorbed in the polymer, as described in the literature, where this interaction has been studied using experimental or theoretical methods [38–43].

Table 1. Experimental results of SCCO₂ density, equilibrium sorption mass gain fraction (M_{∞}), desorption diffusivity (D_d), and sorption diffusivity (D_s) at various temperatures and pressures.

Pressure (MPa)	Temperature (°C)	SCCO ₂ Density (kg/m ³)	M_{∞} (wt%)	D_d (10 ⁻¹¹ m ² /s)	D_s (10 ⁻¹¹ m ² /s)
20	40	839.8	10.5	1.18	0.13
20	50	784.3	9.8	0.64	0.18
20	60	723.7	9.0	0.40	0.30
30	40	909.9	11.7	1.02	0.11
30	50	870.4	10.8	0.79	0.24
30	60	829.7	10.3	0.71	0.22
40	40	956.1	12.8	1.47	0.12
40	50	923.3	12.0	1.20	0.12
40	60	890.1	11.0	0.61	0.26

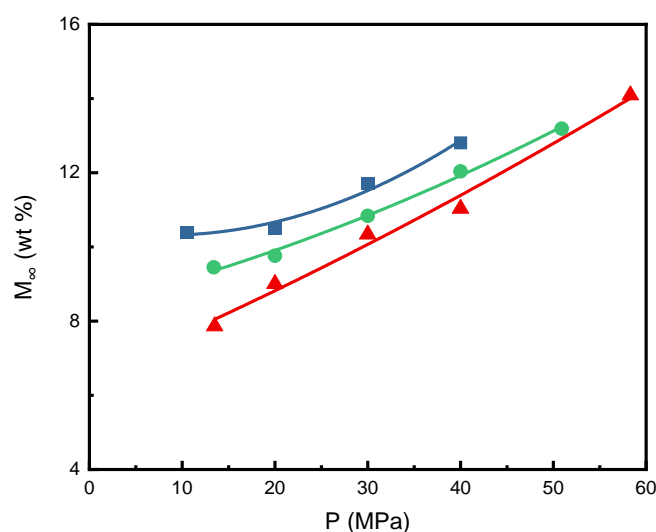


Figure 3. Plot of the equilibrium sorption mass gain fraction of SCCO₂ (M_{∞}) against pressure at various temperatures: ■, 40 °C; ●, 50 °C; ▲, 60 °C.

2.2. The Sorption Mechanism of SCCO₂ in PEI

Furthermore, Figure 4 shows a plot of M_{∞} versus SCCO₂ density for the three isotherms in this study, where concave upward curves were observed. The continuous curves in Figure 4 were obtained by optimal regression of the experimental results. The crossover phenomena is observed in Figure 4. According to the previous literature studies [44,45], the change in the slope of the isotherm shown in Figure 4 may indicate that the PEI polymer has been plasticized. Figure 4 also shows the crossover point with a SCCO₂ density of approximately 840 kg/m³. At lower densities below the crossover point, the solubility of SCCO₂ in PEI decreased with increasing temperature. SCCO₂ solubility increased with temperature when the density was above the crossover point. When the SCCO₂ density exceeds 840 kg/m³, the 40 and 50 °C isotherms are close to each other, but the 50 °C data are still slightly higher than the 40 °C data. The same concave upward

curves of SCCO₂ solubility isotherms were also found in previous studies for polymers of PC and poly (ethylene terephthalate) (PET) [24,44].

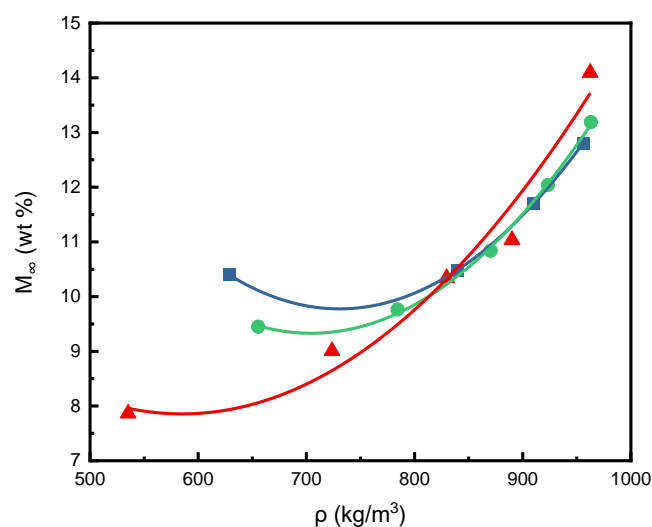


Figure 4. Plot of the equilibrium sorption mass gain fraction of SCCO₂ (M_{∞}) against SCCO₂ density at various temperatures: ■, 40 °C; ●, 50 °C; ▲, 60 °C.

Crossover phenomena show the transfer of sorption mechanisms in polymers of different density states. Gas sorption in polymers has been discussed and reviewed through various physical and mathematical models [46–49]. Experimentally measured gas sorption and desorption data in polymers can be interpreted based on these theoretical considerations. In the lower-density region of SCCO₂, the CO₂ molecular sorption model was dominated by the solubility of CO₂ in the glassy state of the polymer. The density or solvent power was higher for SCCO₂ at lower temperatures, leading to a larger equilibrium sorption mass gain fraction (M_{∞}). When the SCCO₂ density exceeded the crossover point or the penetration concentration [44] where the glass transition occurred, the mobility of the polymer chains increased to a higher degree due to the greater sorption of SCCO₂. With increasing temperature, more plasticization effects existed in higher density regions, as shown in Figure 4. Similar crossover behavior was also expressed in the literature on SCCO₂ sorption in PC and PET [24,44]. In the lower-density region, it is assumed that dual-mode absorption was appropriate for the mass transfer mechanism, where SCCO₂ was absorbed up to the second layer of the polymer substrate. At higher densities beyond the crossover point, the polymer may transit from a glassy to a rubbery state, producing a Fickian diffusion pattern. However, the crossover density value depends on the glass transition temperature (T_g) of the various polymers. PET had a crossover density of approximately 400 kg/m³ and a T_g of approximately 75 °C [44,50], while PC had a crossover density of approximately 680 kg/m³ and a T_g of approximately 150 °C [21,51,52]. The measured T_g of the PEI sample used in this study was approximately 217 °C, consistent with the literature data [53]. Due to the higher T_g , PEI reasonably corresponded to a higher crossover density of 840 kg/m³.

2.3. Comparison of SCCO₂ Diffusivities in Various Polymers

According to Equation (5) presented in Section 3.3, the desorption diffusivity D_d was evaluated from the linear slope values from the plots of (M_d/M_s) against $(t_d)^{1/2}$. The plot of D_d against M_{∞} is shown in Figure 5 for three temperatures with the experimental data obtained in this study. The continuous curve in Figure 5 was obtained by optimal regression of the experimental results. It is observed from Figure 5 that the desorption diffusivities increased significantly with increasing equilibrium SCCO₂ mass gain fraction in the PEI polymer substrate. Under the conditions of 40 °C and 40 MPa, the D_d of SCCO₂ in the PEI matrix was 1.47×10^{-11} m²/s, in which the sorption mass gain fraction

of SCCO₂ was 12.8 wt%. The D_d measured in this study at 60 °C and 13.5 MPa was 0.23×10^{-11} m²/s, in which the sorption mass gain fraction of SCCO₂ was 7.9 wt%. This trend is in agreement with the results of the literature on SCCO₂ desorption in PVC, PC, and PSF polymers [24,25,37].

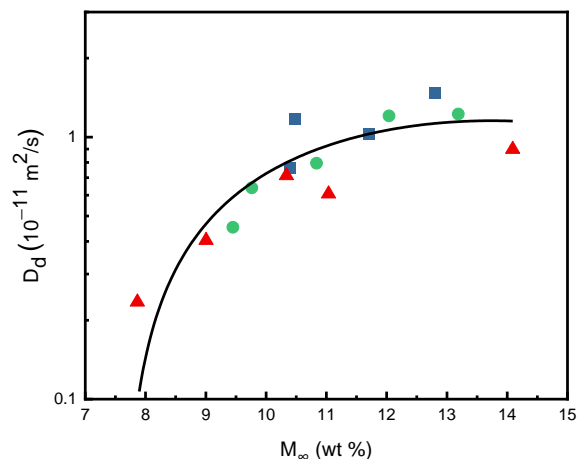


Figure 5. Plot of desorption diffusivity (D_d) versus SCCO₂ equilibrium mass gain fraction at various temperatures: ■, 40 °C; ●, 50 °C; ▲, 60 °C.

As given in Table 1, D_s values increased with temperature but had relatively little dependence on pressure. The largest D_s value was 0.30×10^{-11} m²/s at 60 °C and 20 MPa. Sorption at higher temperatures accelerated CO₂ molecules to fill into the sites of the polymer substrate with higher kinetic energy and, therefore, increased D_s . Due to higher polymer chain mobility at higher temperatures, the driving force of mass transfer would rise, and the drag force for the motion of CO₂ molecules in the polymer would decrease.

PEI exhibited the lowest sorption and desorption diffusivities compared to PC and PSF, which may be due to the physical properties of these polymers. The glass transition temperature of PEI is up to 217 °C [53], which is higher than 150 °C for PC [21,51,52] and 185 to 187 °C for PSF [54,55]. Studies have also found that the yield strength of PEI was 100 to 110 MPa (room temperature) [56,57]. The yield strengths of PC and PSF were approximately 65 MPa and 75 MPa, respectively [58,59]. It can also be observed from Table 1 that the D_d values were greater than D_s , and other polymers of PSF and PC also showed a similar trend [24,25]. During the sorption process, dissolved CO₂ must overcome the interaction forces between polymer chains. The desorption process was carried out under atmospheric pressure; there was a significant pressure drop, and the polymer matrix has also been plasticized during the sorption process. This is the reason why D_d is larger than D_s for PC, PSF, and PEI polymers. However, Muth et al. [37] reported that D_s values were larger than D_d for PVC polymer. This might be due to the fact that PVC has relatively smaller yield strength (about 45 MPa) and lower T_g (about 82 °C) [60], which was favorable for gas sorption.

2.4. Plasticization Effect for the Sorption of SCCO₂ in PEI

Plasticization refers to changes in a given polymer's thermal or mechanical properties, including a decrease in its stiffness and a decrease in its glass transition temperature. Polymer processing using SCCO₂ allows for control of polymer properties such as viscosity and plasticity. In the above discussion of the sorption and desorption diffusivities of CO₂ in PC, PSF, and PEI, the plasticization effect of absorbed CO₂ explains the differences in diffusivity values. During the sorption process, the polymer matrix initially existed in a state of entangled bonds. CO₂ required a stronger driving force for mass transfer to overcome the greater resistance due to the lower mobility of the polymer chains. During desorption, the polymer matrix was swollen and plasticized by CO₂ to have higher chain

mobility. CO₂ molecules experienced less resistance, thereby increasing the desorption rate of CO₂ from the polymer matrix. The existence of CO₂ in PEI was qualitatively investigated in this study by examining the characteristic FTIR spectra. Figure 6 compares the FTIR spectra of untreated PEI and PEI desorbed for 24 h after SCCO₂ sorption treatment for 12 h at 20 MPa and 40 °C. The trapped CO₂ within the PEI specimen can be observed from the spectra with the CO₂ bending mode (ν_2) near 660 cm⁻¹ and the antisymmetric stretching mode (ν_3) near 2340 cm⁻¹.

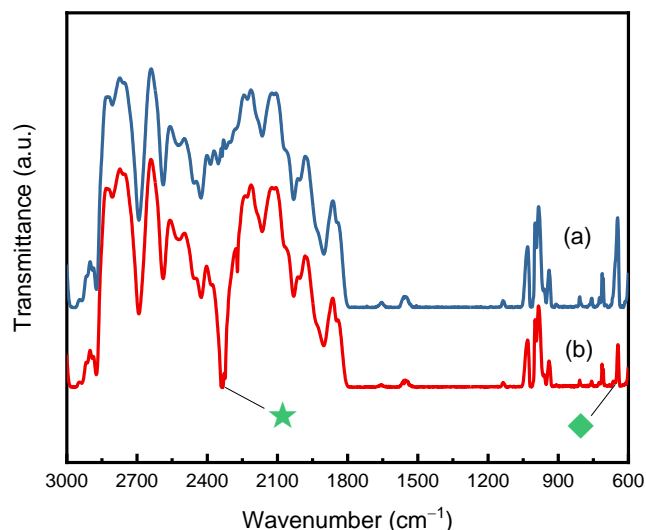


Figure 6. FTIR spectra for the antisymmetric stretching mode (ν_3) for: (a) untreated PEI; and (b) the SCCO₂-treated PEI after 24 h of desorption. (The sorption process was operated at 20 MPa, 40 °C for 12 h. The green symbols represent wavenumbers at 2340 cm⁻¹ and 660 cm⁻¹, respectively).

Figure 7 shows the antisymmetric stretching pattern (ν_3) around 2340 cm⁻¹ for trapped CO₂ in PEI specimens at different desorption times. Spectra (a) and (i) represent FTIR results for pure gaseous CO₂ and PEI, respectively. As shown in spectra (b) to (d), the bands appear to have very broad widths over the desorption interval of 120 s to 4 h. As the desorption time increased, the decrease in transmission bandwidth indicated the desorption of CO₂ from PEI. The IR transmittance shows that CO₂ still existed in the PEI substrate 72 h after being discharged from the high-pressure cell, and the peak in the spectrum (g) still appeared near the wavenumber at 2340 cm⁻¹. The phenomena in Figure 7 qualitatively shows that CO₂ remained in PEI after various desorption times.

The SEM images of the untreated PEI and the SCCO₂-treated PEI (under the process condition of 40 °C, 20 MPa, and sorption time for 12 h) are presented in Figure 8. Compared to the untreated PEI in Figure 8a, microstructure change and surface deformation were observed for SCCO₂-treated PEI in Figure 8b. This morphology change also qualitatively implies the plasticization effect during the sorption and desorption of SCCO₂ in PEI.

Figure 9 shows loss modulus curves of (a) untreated PEI, (b) PEI after sorption in SCCO₂ at 20 MPa and 40 °C for 12 h, and (c) PEI under previous SCCO₂-treated conditions that had been depressurized in the atmosphere for more than one month. The maximum loss modulus of untreated PEI was 233 °C, while that of treated PEI was 227 °C. This shift in loss maxima was attributed to the plasticization of the PEI substrate with the increase in polymer chain mobility. This result also corresponds to the fact that D_d was greater than D_s for SCCO₂ in PEI. Moreover, when the SCCO₂-treated PEI was depressurized for over one month, the maximum loss modulus returned to 232 °C, nearly the same as untreated PEI. It indicated that SCCO₂ left no residual in PEI after a long time of depressurization and would have little effect on PEI's properties.

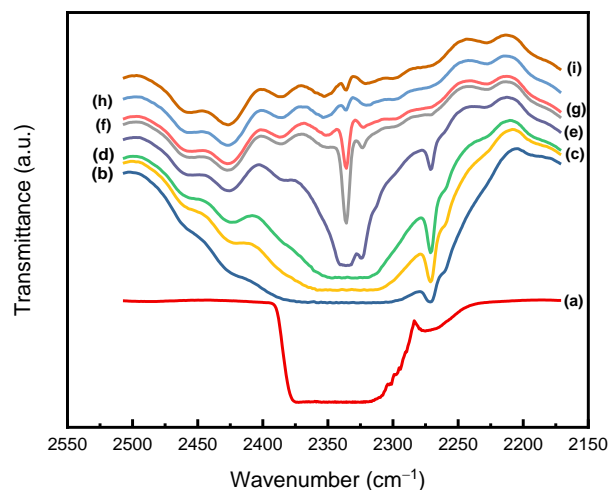


Figure 7. FTIR spectra for the antisymmetric stretching mode (ν_3) of CO_2 for (a) gaseous CO_2 ; (i) untreated PEI; and the CO_2 entrapped within PEI film after various desorption times of (b) 120 s; (c) 1 h; (d) 4 h; (e) 24 h; (f) 48 h; (g) 72 h; and (h) 96 h. (The sorption process was operated at 20 MPa, 40 °C for 12 h).

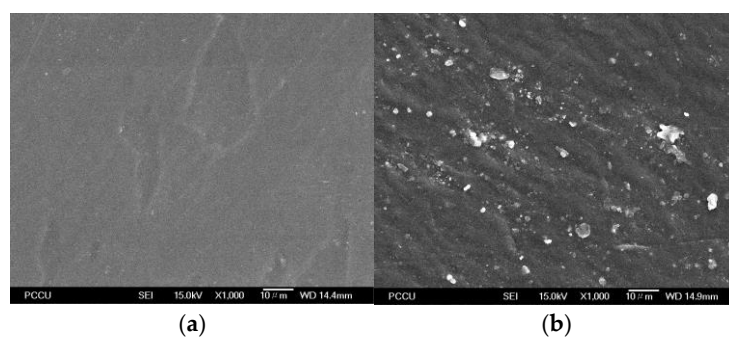


Figure 8. The SEM images of (a) untreated PEI and (b) SCCO_2 -treated PEI at 40 °C, 20 MPa, and sorption time of 12 h.

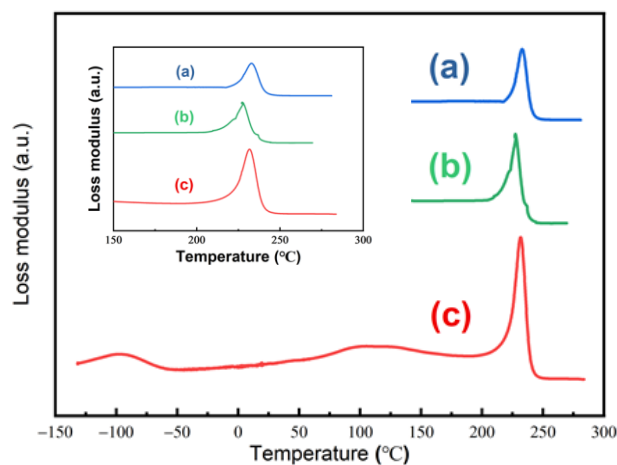


Figure 9. Loss modulus as a function of the temperature of PEI for: (a) untreated; (b) treated with SCCO_2 at 20 MPa and 40 °C for 12 h; (c) more than one month of desorption with the same treated conditions as (b).

3. Materials and Methods

3.1. Material

Polyetherimide (PEI, CAS registry number 61128-46-9, molecular formula $(C_{37}H_{24}N_2O_6)_n$, melt index 9 g/10 min (at 337 °C, 6.6 kg), density 1.27 g/cm³, glass transition temperature 217 °C) was purchased from Sigma-Aldrich, UNI-ONWARD Corp., New Taipei City, Taiwan. The structure of PEI is shown in Figure 10. PEI was hot pressed at 240 °C and then cut into dimensions of 40 mm × 10 mm. The membrane sample with a thickness of 0.6 mm for experimental sorption measurements and the membrane samples with a thickness of 0.2 mm were used for FTIR and loss modulus experiments. CO₂ was purchased from San-Fu Chemical Company, Taiwan, with a certified purity greater than 99.8%. All chemicals were used as received.

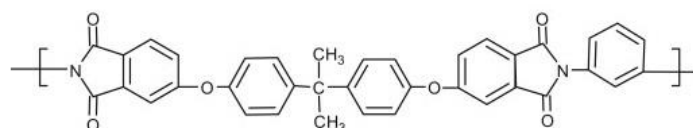


Figure 10. The structure of polyetherimide (PEI).

3.2. Apparatus and Procedures

The experimental equipment is shown in Figure 11. The CO₂ was stored in the cylinder and compressed to the operating pressure by a syringe pump (ISCO, model 100DX, ISCO, Lincoln, NE, USA). The PEI specimen was weighed using a digital balance (Mettler AE200, Greifensee, Switzerland, sensitivity 0.1 mg) prior to putting it into a stainless steel high-pressure cell with an inner diameter of 5/8 inch and capacity of 10 cm³. The high-pressure cell was maintained at a desired temperature using a constant temperature bath (ISCO, SFX2-10).

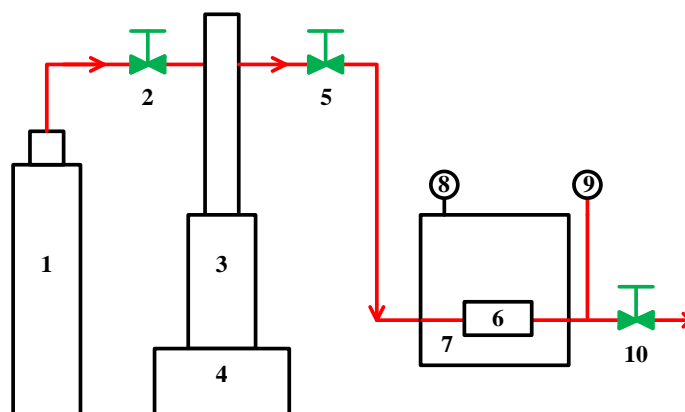


Figure 11. Schematic diagram of the experiment apparatus. 1. CO₂ gas cylinder; 2. check valve; 3. high pressure syringe pump; 4. temperature and pressure controller; 5. needle valve; 6. high pressure equilibrium cell; 7. constant temperature bath; 8. temperature indicator; 9. pressure indicator; 10. needle valve.

At the beginning of the ex situ gravimetric experiment, the original PEI specimen was weighed using a digital balance to record its initial weight, M_0 . The high-pressure cell was purged with pure CO₂ to remove any air inside. Then, with the outlet valve closed, pressurized CO₂ from the ISCO injection pump was charged into the high-pressure equilibrium cell. The equilibrium cell reached the preset equilibrium pressure within 10 s.

The pressure and temperature in the cell were dynamically controlled throughout the sorption experiments. After a certain period of sorption time, the cell was depressurized, and the specimen was rapidly taken onto the digital balance at room temperature under atmospheric pressure. The originally dissolved CO₂ in the PEI specimen was desorbed as

pressure was released. The PEI specimen's weight was recorded by the digital balance as a function of time. Normally, it takes 30 s during the depressurization process before the digital balance records the first data. At desorption time t_d , the weight of the PEI membrane was M . The mass gain fraction was calculated by

$$\text{Mass gain fraction (wt\%)} = \frac{M - M_0}{M_0} \times 100\% \quad (1)$$

During the desorption process, the weight of the PEI sample was measured at every 10-s interval for at least 120 s. These measurement procedures were similar to those in the previous literature, where the ex situ gravimetric method was applied [24,25]. A PEI sample sheet was used only once at a specific sorption temperature, pressure, and sorption time. A number of PEI sample sheets were prepared and used in this study. The weight of the PEI sample decreased with the prolongation of desorption time, and the mass gain fraction curve showed a linear decreasing trend with the square root of desorption time within the first 100 s. A schematic sorption and desorption diagram is shown in Figure 12.

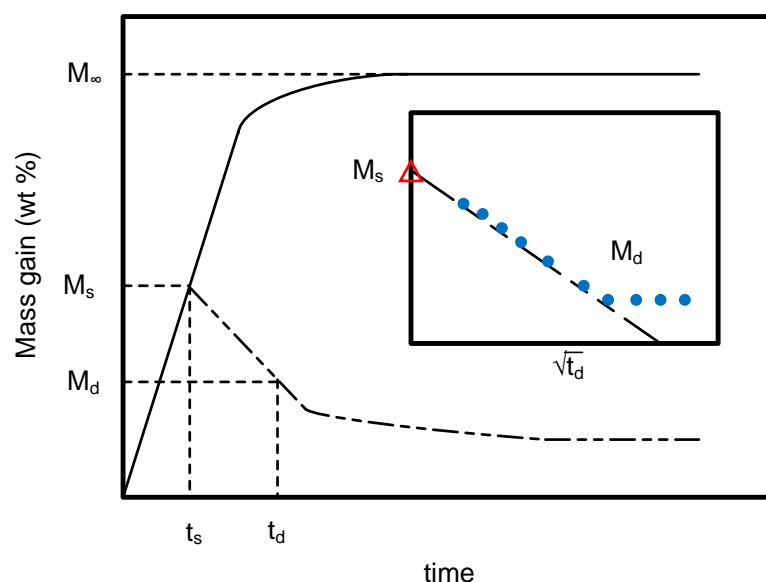


Figure 12. Schematic illustration for the sorption (—) and desorption (---) profiles. The inserted graph shows that the mass gain fraction decreased linearly with the square root of the initial desorption time.

It is presented in Figure 12 that at a sorption or soaking time t_s , the mass gain fraction of the PEI specimen owing to the sorption of CO_2 was M_s . In the desorption process, the mass gain fraction decreased with the extension of desorption time and became M_d at a certain desorption time t_d . For an initial desorption time of about 100 s, the reduction in mass gain fraction is almost a linear function of the square root of the desorption time t_d , as shown by the graph inserted in Figure 12. The M_s value was determined by extrapolating the linear portion of the initial desorption curve to zero desorption time, as shown by the point M_s (with the symbol Δ) in the graph inserted in Figure 12. At a long enough sorption time, the mass gain fraction reached its saturation value M_∞ corresponded to the equilibrium mass gain fraction of SCCO_2 at the given experimental temperature, pressure, and sorption time. These data were then utilized to calculate sorption and desorption diffusivities of SCCO_2 in polymer. A FTIR spectrometer (Digilab FTS-3000, Burladingen, Germany) at room temperature and atmospheric pressure with a resolution of 2 cm^{-1} was used to analyze the transmittance bands of CO_2 in the PEI specimen. A loss modulus analysis (TA instruments DMA2980, New Castle, DE, USA) was used to determine the shifting of loss maxima for pure and SCCO_2 -treated PEI specimens.

3.3. Data Analysis Method

The analyses of sorption and desorption of SCCO₂ in polymer have been presented in the previous literature [14,23–25], based on the mathematical model investigated by Fick. According to the one-dimension Fickian diffusion model, the governing equation for the mass transfer of SCCO₂ in a plane sheet polymer is

$$\frac{\partial C}{\partial t} = D \frac{\partial^2 C}{\partial X^2} \quad (2)$$

where C is the CO₂ concentration in PEI, and the CO₂ diffusivity D is assumed to be constant at a specific temperature and pressure. The solution to Equation (2) is based on the assumption of semi-infinite or one-dimensional sheets in most cases. According to the literature, for thin flat membrane geometries, the thickness-to-length ratio should be less than 0.16 [20,21]. The ratio in this study was 0.06, which is suitable for applying the one-dimensional solution of Equation (2) without considering the edge effect. Applying the approach of Laplace transform with proper boundary conditions, the solution of Equation (2) is [32]

$$\frac{M_s}{M_\infty} = 1 - \frac{8}{\pi^2} \sum_{n=0}^{\infty} \frac{1}{(2n+1)^2} \exp\left[\frac{-(2n+1)^2 \pi^2 D_s t_s}{l^2}\right] \quad (3)$$

where l is the thickness of the PEI sample membrane, D_s is the sorption diffusivity, M_s and M_∞ are the sorption mass gain fraction at sorption time t_s and the equilibrium sorption mass gain fraction, respectively. For a long sorption process, Equation (3) is simplified as

$$\frac{M_s}{M_\infty} = 1 - \frac{8}{\pi^2} \exp\left[\frac{-\pi^2 D_s t_s}{l^2}\right] \quad (4)$$

The sorption diffusivity D_s can thus be evaluated by plotting of $\ln [1 - (M_s/M_\infty)]$ against t_s/l^2 .

Equation (2) can also be used to solve the desorption process for a thin flat film polymer. After simplifying the solution to a short desorption time t_d , the mass gain fraction of desorption M_d is expressed by

$$\frac{M_d}{M_s} = -\frac{4}{l} \sqrt{\frac{D_d t_d}{\pi}} \quad (5)$$

where D_d is the diffusivity for desorption. As mentioned above, the M_s value is determined by extrapolating the linear portion of the short-time desorption curve to zero desorption time. The short time period desorption diffusivity D_d can also be obtained from data plotting the desorption mass gain fraction (M_d/M_s) versus $(t_d)^{1/2}$.

4. Conclusions

In this study, the sorption and diffusion experiments of SCCO₂ in 0.6 mm thick PEI membrane samples were conducted in the temperature and pressure ranges of 40 to 60 °C and 20 to 40 MPa, respectively. A high-pressure equilibrium cell and the ISCO units were used in this study. The sorption amounts under different operating conditions were determined using an ex situ gravimetric method. The sorption and desorption diffusivities were evaluated using the Fickian diffusion model. The equilibrium sorption mass gain fraction depended on the process conditions and reached the value of 12.8 wt% at 40 °C and 40 MPa. The sorption diffusivity increased with temperature and was slightly pressure-dependent. Due to the plasticization effect, the desorption diffusivity was greater than the sorption diffusivity in PEI. The plot of sorption mass gain fractions at isotherms against SCCO₂ density showed a crossover point at the SCCO₂ density of approximately 840 kg/m³. The result indicated changes in the mass transfer mechanism at the crossover point. This

study compared the crossover densities of different polymers and derived the dependence of the glass transition temperatures and yield strengths of different polymer substrates. The desorption of CO₂ from PEI was also qualitatively studied using FTIR spectroscopy, and a decrease in absorbed CO₂ in the PEI polymer was observed with increasing desorption time. This study examined the shift in the loss modulus maxima and the SEM images of SCCO₂-treated PEI, which was indicative of plasticization on PEI induced by SCCO₂ sorption.

Author Contributions: W.-H.H.: data curation, writing—original draft. P.-H.C.: conceptualization, validation, writing—original draft. C.-W.C.: methodology, investigation, validation, supervision, funding acquisition. C.-S.S.: investigation, validation, supervision. M.T.: funding acquisition, conceptualization, supervision, writing—editing. J.-C.T.: validation. Y.-P.C.: supervision, writing—review and editing. F.-H.L.: investigation, validation. W.-H.H. and P.-H.C. contributed equally to this work. All authors have read and agreed to the published version of the manuscript.

Funding: This work was supported by the National Science and Technology Council of Taiwan (NSTC 113-2221-E-027-002), and the University System of Taipei Joint Research Program of USTP-NTUT-NTOU-113-04.

Institutional Review Board Statement: Not applicable.

Informed Consent Statement: Not applicable.

Data Availability Statement: The data are contained within the article.

Conflicts of Interest: The authors declare that they have no conflicts of interests. The authors declare no competing financial interests.

References

1. Mensitieri, G.; Scherillo, G.; La Manna, P.; Musto, P. Sorption thermodynamics of CO₂, H₂O, and CH₃OH in a glassy polyetherimide: A molecular perspective. *Membranes* **2019**, *9*, 23. [\[CrossRef\]](#) [\[PubMed\]](#)
2. Galizia, M.; Chi, W.S.; Smith, Z.P.; Merkel, T.C.; Baker, R.W.; Freeman, B.D. 50th Anniversary perspective: Polymers and mixed matrix membranes for gas and vapor separation: A review and prospective opportunities. *Macromolecules* **2017**, *50*, 7809–7843. [\[CrossRef\]](#)
3. Edebali, S. (Ed.) *Advanced Sorption Process Applications*; IntechOpen: London, UK, 2019. [\[CrossRef\]](#)
4. Machado, N.D.; Mosquera, J.E.; Raquel, E.; Martini, R.E.; Goñi, M.L.; Nicol'as, A.; Gañán, N.A. Supercritical CO₂-assisted impregnation/deposition of polymeric materials with pharmaceutical, nutraceutical, and biomedical applications: A review (2015–2021). *J. Supercrit. Fluids* **2022**, *191*, 105763. [\[CrossRef\]](#)
5. Sattari, A.; Ramazani, A.; Aghahosseini, H.; Aroua, M.K. The application of polymer containing materials in CO₂ capturing via absorption and adsorption methods. *J. CO₂ Util.* **2021**, *48*, 101526. [\[CrossRef\]](#)
6. Ansaloni, L.; Alcock, B.; Peters, T.A. Effects of CO₂ on polymeric materials in the CO₂ transport chain: A review. *Int. J. Greenh. Gas Control.* **2020**, *94*, 102930. [\[CrossRef\]](#)
7. Kang, X.; Mao, L.; Shi, J.; Liu, Y.; Zha, B.; Xu, J.; Yuzhou Jiang, Y.; Lichtfouse, E.; Jin, H.; Guo, L. Supercritical carbon dioxide systems for sustainable and efficient dissolution of solutes: A review. *Environ. Chem. Lett.* **2024**, *22*, 815–839. [\[CrossRef\]](#)
8. Prasad, S.K.; Sangwai, J.S.; Byun, H.-S. A review of the supercritical CO₂ fluid applications for improved oil and gas production and associated carbon storage. *J. CO₂ Util.* **2023**, *72*, 102479. [\[CrossRef\]](#)
9. Sarver, J.A.; Kiran, E. Foaming of polymers with carbon dioxide—The year-in-review—2019. *J. Supercrit. Fluids* **2021**, *173*, 105166. [\[CrossRef\]](#)
10. Neděla, O.; Slepčka, P.; Švorčík, V. Surface modification of polymer substrates for biomedical applications. *Materials* **2017**, *10*, 1115. [\[CrossRef\]](#)
11. Khongnakorn, W.; Bootluck, W.; Jutaporn, P. Surface modification of FO membrane by plasma-grafting polymerization to minimize protein fouling. *J. Water Process Eng.* **2020**, *38*, 101633. [\[CrossRef\]](#)
12. Liu, Z.; Song, L.; Dai, X.; Yang, G.; Han, B.; Xu, J. Grafting of methyl methacrylate onto isotactic polypropylene film using supercritical CO₂ as a swelling agent. *Polymer* **2002**, *43*, 1183–1188. [\[CrossRef\]](#)
13. He, T.; He, J.; Wang, Z.; Cui, Z. Modification strategies to improve the membrane hemocompatibility in extracorporeal membrane oxygenator (ECMO). *Adv. Compos. Mater.* **2021**, *4*, 847–864. [\[CrossRef\]](#) [\[PubMed\]](#)
14. Chen, P.-H.; Iun, C.-P.; Tsai, J.-C.; Tang, M. Grafting of 2-hydroxyethyl methacrylate onto polyacrylonitrile using supercritical carbon dioxide. *J. Supercrit. Fluids* **2022**, *186*, 105589. [\[CrossRef\]](#)
15. Ricci, E.; De Angelis, M.G.; Minelli, M. A comprehensive theoretical framework for the sub and supercritical sorption and transport of CO₂ in polymers. *Chem. Eng. J.* **2022**, *435*, 135013. [\[CrossRef\]](#)
16. Wang, D.; Cai, Z.; Huang, X.; Wang, L. Study on the dissolution and diffusion of supercritical carbon dioxide in polystyrene melts based on adsorption and diffusion mechanism. *ACS Omega* **2021**, *6*, 1971–1984. [\[CrossRef\]](#)

17. Goñi, M.L.; Gañán, N.A.; Martini, R.E.; Strumia, M.C. Mass transfer kinetics and diffusion coefficient estimation of bioinsecticide terpene ketones in LDPE films obtained by supercritical CO₂-assisted impregnation. *J. Appl. Polym. Sci.* **2017**, *134*, 45558. [CrossRef]
18. Ma, Z.; Zhang, G.; Shi, X.; Yang, Q.; Li, J.; Liu, Y.; Fan, X. Microcellular foaming of poly(phenylene sulfide)/poly(ether sulfones) blends using supercritical carbon dioxide. *J. Appl. Polym. Sci.* **2015**, *132*, 42634. [CrossRef]
19. Burges, S.; Kriegel, R.M.; Koros, W.J. Carbon dioxide sorption and transport in amorphous poly(ethylene furanoate). *Macromolecules* **2015**, *48*, 2184–2193. [CrossRef]
20. Lin, S.; Yang, J.; Yan, J.; Zhao, Y.; Yang, B. Sorption and diffusion of supercritical carbon dioxide in a biodegradable polymer. *J. Macromol. Sci. Phys.* **2010**, *49*, 286–300. [CrossRef]
21. Zhao, J.J.; Zhao, Y.P.; Yang, B. Investigation of sorption and diffusion of supercritical carbon dioxide in polycarbonate. *J. Appl. Polym. Sci.* **2008**, *109*, 1661–1666. [CrossRef]
22. Pantoula, M.; Panayitou, C. Sorption and swelling in glassy polymer/carbon dioxide systems: Part I. Sorption. *J. Supercrit. Fluids* **2006**, *37*, 254–262. [CrossRef]
23. Duarte, A.R.C.; Martins, C.; Coimbra, P.; Gil, M.H.M.; de Sousa, H.C.; Duarte, C.M.M. Sorption and diffusion of dense carbon dioxide in a biocompatible polymer. *J. Supercrit. Fluids* **2006**, *38*, 392–398. [CrossRef]
24. Tang, M.; Du, T.B.; Chen, Y.P. Sorption and diffusion of supercritical carbon dioxide in polycarbonate. *J. Supercrit. Fluids* **2004**, *28*, 207–218. [CrossRef]
25. Tang, M.; Huang, Y.C.; Chen, Y.P. Sorption and diffusion of supercritical carbon dioxide into polysulfone. *J. Appl. Polym. Sci.* **2004**, *94*, 474–482. [CrossRef]
26. Tomasko, D.L.; Li, H.; Liu, D.; Han, X.; Wingert, M.J.; Lee, L.J.; Koelling, K.W. A review of CO₂ applications in the processing of polymers. *Ind. Eng. Chem. Res.* **2003**, *42*, 6431–6456. [CrossRef]
27. Seifert, B.; Mihanetzis, G.; Groth, T.; Albrecht, W.; Richau, K.; Missirlis, Y.; Paul, D.; von Sengbrusch, G. Polyetherimide: A new membrane-forming polymer for biomedical applications. *Artif. Organs* **2002**, *26*, 189–199. [CrossRef] [PubMed]
28. Feng, D.; Li, L.; Wang, Q. Fabrication of three-dimensional polyetherimide bead foams via supercritical CO₂/ethanol cofoaming technology. *RSC Adv.* **2019**, *9*, 4072–4081. [CrossRef]
29. Aher, B.; Olson, N.M.; Kumar, V. Production of bulk solid-state PEI nanofoams using supercritical CO₂. *J. Mater. Res.* **2013**, *28*, 2366–2373. [CrossRef]
30. Zhou, C.; Vaccaro, N.; Sundarram, S.S.; Li, W. Fabrication and characterization of polyetherimide nanofoams using supercritical CO₂. *J. Cell. Plast.* **2012**, *48*, 239–255. [CrossRef]
31. Liu, W.; Ma, J.; Wang, D.; Wang, P.; Zhao, J.; Wenzheng Wu, W.; Song, W. Performance modulation and 3D printing parameters optimization of implantable medical tricalcium-silicate/polyetherimide composite. *Ceram. Int.* **2021**, *47*, 10679–10687. [CrossRef]
32. Crank, J. *Mathematics of Diffusion*, 2nd ed.; Oxford University Press: Oxford, UK; Elsevier: Amsterdam, The Netherlands, 1975.
33. NIST Chemistry WebBook, SRD 69. Available online: <https://webbook.nist.gov/cgi/cbook.cgi?ID=C124389> (accessed on 20 August 2024).
34. Brantley, N.H.; Kazarian, S.G.; Eckert, C.A. In situ FTIR measurement of carbon dioxide sorption into poly(ethylene terephthalate) at elevated pressures. *J. Appl. Polym. Sci.* **2000**, *77*, 764–775. [CrossRef]
35. Kazarian, S.G.; Vincent, M.F.; Bright, F.V.; Liotta, C.L.; Eckert, C.A. Specific inter-molecular interaction of carbon dioxide with polymers. *J. Am. Chem. Soc.* **1996**, *118*, 1729–1736. [CrossRef]
36. Nelson, M.R.; Borkman, R.F. Ab initio calculations on CO₂ binding to carbonyl groups. *J. Phys. Chem.* **1998**, *102*, 7860–7863. [CrossRef]
37. Muth, O.; Hirth, T.; Vogel, H. Investigation of sorption and diffusion of supercritical carbon dioxide into poly(vinyl chloride). *J. Supercrit. Fluids* **2001**, *19*, 299–306. [CrossRef]
38. Bos, A.; Punt, I.G.M.; Wessling, M. CO₂-induced plasticization phenomena in glassy polymers. *J. Membr. Sci.* **1999**, *155*, 67–78. [CrossRef]
39. Shieh, Y.T.; Su, J.H.; Manivannan, G.; Lee, P.H.C.; Sawan, S.P.; Spall, W.D. Interaction of supercritical carbon dioxide with polymers. II. Amorphous polymers. *J. Appl. Polym. Sci.* **1996**, *59*, 707–717. [CrossRef]
40. Wang, J.; Wang, M.; Hao, J.; Fujita, S.-I.; Arai, M.; Wu, Z.; Zhao, F. Theoretical study on interaction between CO₂ and carbonyl compounds: Influence of CO₂ on infrared spectroscopy and activity of C=O. *J. Supercrit. Fluids* **2010**, *54*, 9–15. [CrossRef]
41. Yuan, Y.; Teja, A.S. Quantification of specific interactions between CO₂ and the carbonyl group in polymers via ATR-FTIR measurements. *J. Supercrit. Fluids* **2011**, *56*, 208–212. [CrossRef]
42. Petrovic, B.; Gorbounov, M.; Soltani, S.M. Influence of surface modification on selective CO₂ adsorption: A technical review on mechanisms and methods. *Microporous Mesoporous Mater.* **2021**, *312*, 110751. [CrossRef]
43. Gabrienko, A.A.; Ewing, A.V.; Andrey, M.; Chibiryaev, A.M.; Alexander, M.; Agafontsev, A.M.; Konstantin, A.; Dubkov, K.A.; Kazarian, S.G. New insights into the mechanism of interaction between CO₂ and polymers from thermodynamic parameters obtained by in situ ATR-FTIR spectroscopy. *Phys. Chem. Chem. Phys.* **2016**, *18*, 6465–6475. [CrossRef]
44. von Schnitzler, J.; Eggers, R. Mass transfer in polymers in a supercritical CO₂-atmosphere. *J. Supercrit. Fluids* **1999**, *16*, 81–92. [CrossRef]

45. Pierleon, D.; Minelli, M.; Scherillo, G.; Mensitieri, G.; Loianno, W.; Bonavolonta, F.; Doghieri, F. Analysis of a polystyrene—Toluene system through “dynamic” sorption tests: Glass transition and retrograde vitrification. *J. Phys. Chem. B* **2017**, *121*, 9969–9981. [[CrossRef](#)] [[PubMed](#)]
46. Kim, J.; Kim, K.H.; Ryu, Y.; Cha, S.W. Modeling and experiment for the diffusion coefficient of subcritical carbon dioxide in poly(methyl methacrylate) to predict gas sorption and desorption. *Polymers* **2022**, *14*, 596. [[CrossRef](#)]
47. Kiran, E.; Sarver, J.A.; Hassler, J.C. Solubility and diffusivity of CO₂ and N₂ in polymers and polymer swelling, glass transition, melting, and crystallization at high pressure: A critical review and perspectives on experimental methods, data, and modeling. *J. Supercrit. Fluids* **2022**, *185*, 105378. [[CrossRef](#)]
48. Minelli, M.; Sarti, G.C. 110th Anniversary: Gas and vapor sorption in glassy polymeric membranes-critical review of different physical and mathematical models. *Ind. Eng. Chem. Res.* **2020**, *59*, 341–365. [[CrossRef](#)]
49. Wang, L.; Corriou, J.-P.; Castel, C.; Favre, E. Transport of gases in glassy polymers under transient conditions: Limit-behavior investigations of dual-mode sorption theory. *Ind. Eng. Chem. Res.* **2013**, *52*, 1089–1101. [[CrossRef](#)]
50. Silva, E.; Fedel, M.; Deflorian, F.; Cotting, F.; Lins, V. Properties of post-consumer polyethylene terephthalate coating mechanically deposited on mild steels. *Coatings* **2019**, *9*, 28. [[CrossRef](#)]
51. Song, P.; Trivedi, A.R.; Siviour, C.R. Mechanical response of four polycarbonates at a wide range of strain rates and temperatures. *Polym. Test.* **2023**, *121*, 107986. [[CrossRef](#)]
52. Palczynski, K.; Wilke, A.; Paeschke, M.; Dzubiella, J. Molecular modeling of polycarbonate materials: Glass transition and mechanical properties. *Phys. Rev. Mater.* **2017**, *1*, 043804. [[CrossRef](#)]
53. Zhang, Q.; Chen, X.; Zhang, B.; Zhang, T.; Lu, W.; Chen, Z.; Liu, Z.; Kim, S.H.; Donovan, B.; Warzoha, R.J.; et al. High-temperature polymers with record-high breakdown strength enabled by rationally designed chain-packing behavior in blends. *Matter* **2021**, *4*, 2448–2459. [[CrossRef](#)]
54. Murakami, K.; Kudo, H. Gamma-rays irradiation effects on polysulfone at high temperature. *Nucl. Instrum. Methods Phys. Res. B* **2007**, *265*, 125–129. [[CrossRef](#)]
55. Mushtaq, A.; Mukhtar, H.B.; Shariff, A.M. Effect of Glass Transition Temperature in Enhanced Polymeric Blend Membranes. *Procedia Eng.* **2016**, *148*, 11–17. [[CrossRef](#)]
56. Kim, K.-Y.; Ye, L.; Yan, C. Fracture Behavior of Polyetherimide (PEI) and Interlaminar Fracture of CF/PEI Laminates at Elevated Temperatures. *Polym. Compos.* **2005**, *26*, 20–28. [[CrossRef](#)]
57. Sun, Z.; Li, Y.Q.; Huang, P.; Cao, H.-J.; Zeng, W.; Li, J.; Li, F.; Sun, B.-G.; Shi, H.-Q.; Zhou, Z.-L.; et al. Temperature-dependent mechanical properties of polyetherimide composites reinforced by graphene oxide-coated short carbon fibers. *Compos. Struct.* **2021**, *270*, 114075. [[CrossRef](#)]
58. Cao, K.; Ma, X.; Zhang, B.; Wang, Y.; Wang, Y. Tensile behavior of polycarbonate over a wide range of strain rates. *Mater. Sci. Eng. A* **2010**, *527*, 4056–4061. [[CrossRef](#)]
59. Chukov, D.; Nematulloev, S.; Zadorozhnyy, M.; Victor Tcherdyntsev, V.; Stepashkin, A.; Zhrebtsov, D. Structure, mechanical and thermal properties of polyphenylene sulfide and polysulfone impregnated carbon fiber composites. *Polymers* **2019**, *11*, 684. [[CrossRef](#)]
60. Xie, X.-L.; Liu, Q.-X.; Li, R.K.-Y.; Zhou, X.-P.; Qing-Xin Zhang, Q.-X.; Yu, Z.-Z.; Mai, Y.-W. Rheological and mechanical properties of PVC/CaCO₃ nanocomposites prepared by in situ polymerization. *Polymer* **2004**, *45*, 6665–6673. [[CrossRef](#)]

Disclaimer/Publisher’s Note: The statements, opinions and data contained in all publications are solely those of the individual author(s) and contributor(s) and not of MDPI and/or the editor(s). MDPI and/or the editor(s) disclaim responsibility for any injury to people or property resulting from any ideas, methods, instructions or products referred to in the content.